Evaluation of cataract formation in fish exposed to environmental radiation at Chernobyl and Fukushima

Adélaïde Lerebours, Justyn Regini, Roy A Quinlan, Toshihiro Wada, Barbara Pierscionek, Martin Devonshire, Alexia A Kalligeraki, Alice Uwineza, Laura Young, John M Girkin, et al.

Published Open Access as:

Lerebours, A., Regini, J., Quinlan, R. A., Wada, T., Pierscionek, B., Devonshire, M., ... & Smith, J. T. (2023). Evaluation of cataract formation in fish exposed to environmental radiation at Chernobyl and Fukushima. *Science of the Total Environment*, 165957.

Evaluation of cataract formation in fish exposed to environmental radiation at Chernobyl and Fukushima

Adélaïde Lerebours[1,2], Justyn Regini[3], Roy A. Quinlan[4], Toshihiro Wada[5], Barbara Pierscionek[6], Martin Devonshire[2], Alexia A. Kalligeraki[4], Alice Uwineza[4], Laura Young[4], John M. Girkin[7], Phil Warwick[8], Kurt Smith[9], Masato Hoshino[10], Kentaro Uesugi[10], Naoto Yagi[10], Nick Terrill[11], Olga Shebanova[11], Tim Snow[11] and Jim T. Smith[1*]

[1]School of the Environment, Geography and Geosciences, University of Portsmouth, Portsmouth, PO1 3QL, United Kingdom

[2]School of Biological Sciences, University of Portsmouth, Portsmouth, PO1 2DY, United Kingdom

[3]School of Optometry and Vision Sciences, University of Cardiff, Cardiff, CA10 3AT, United Kingdom.

[4]Department of Biosciences, University of Durham, Upper Mountjoy, Stockton Road, Durham DH1 3LE, United Kingdom.

[5]Institute of Environmental Radioactivity, Fukushima University, 1 Kanayagawa, Fukushima City, Japan.

[6]Medical Technology Research Centre, Anglia Ruskin University, Bishop Hall Lane, Chelmsford, CM1 1SQ, United Kingdom.

[7]Department of Physics, University of Durham, South Road, Durham DH1 3LE, United Kingdom

[8]GAU-Radioanalytical, University of Southampton, NOCS, European way, SO14 6HT Southampton,United Kingdom

[9]Centre for Radiochemistry Research, School of Chemistry, University of Manchester, Oxford Road, Manchester, M13 9PL, UK

[10]Japan Synchrotron Radiation Research Institute (Spring-8), 1-1-1, Kouto, Sayo-cho, Sayo-gun, Hyogo, 679-5198 Japan

[11]Diamond Light Source, Harwell Science & Innovation Campus, Didcot, OX11 0DE, UK

* Corresponding author

Keywords: Radiation; Cataract; Fish; Chernobyl; Fukushima; Radiocaesium; Radiostrontium; Dose; SAXs

Abbreviations: CMOS, Complementary metal-oxide-semiconductor; DMSO, dimethyl sulphoxide; GLM, generalised linear model; HEPES; N-2-hydroxyethylpiperazine-N'-2-ethanesulfonic acid; h, hours; ICRP, International Commission on Radiological Protection; IR, ionising radiation; mGy milli-Gray; PFA, paraformaldehyde; PBS, phosphate buffered saline; SAXS, small angle X-ray scattering.

Highlights

Most detailed analysis of cataract formation in free-living wild animals exposed to radiation

Protein aggregation, epithelial cell density and focal length studied

Epithelial cell density study helps to inform on radiation impacts over time as the lens develops

No evidence found of radiation-related lens opacities

No evidence found of early stage cataract formation

Graphical Abstract

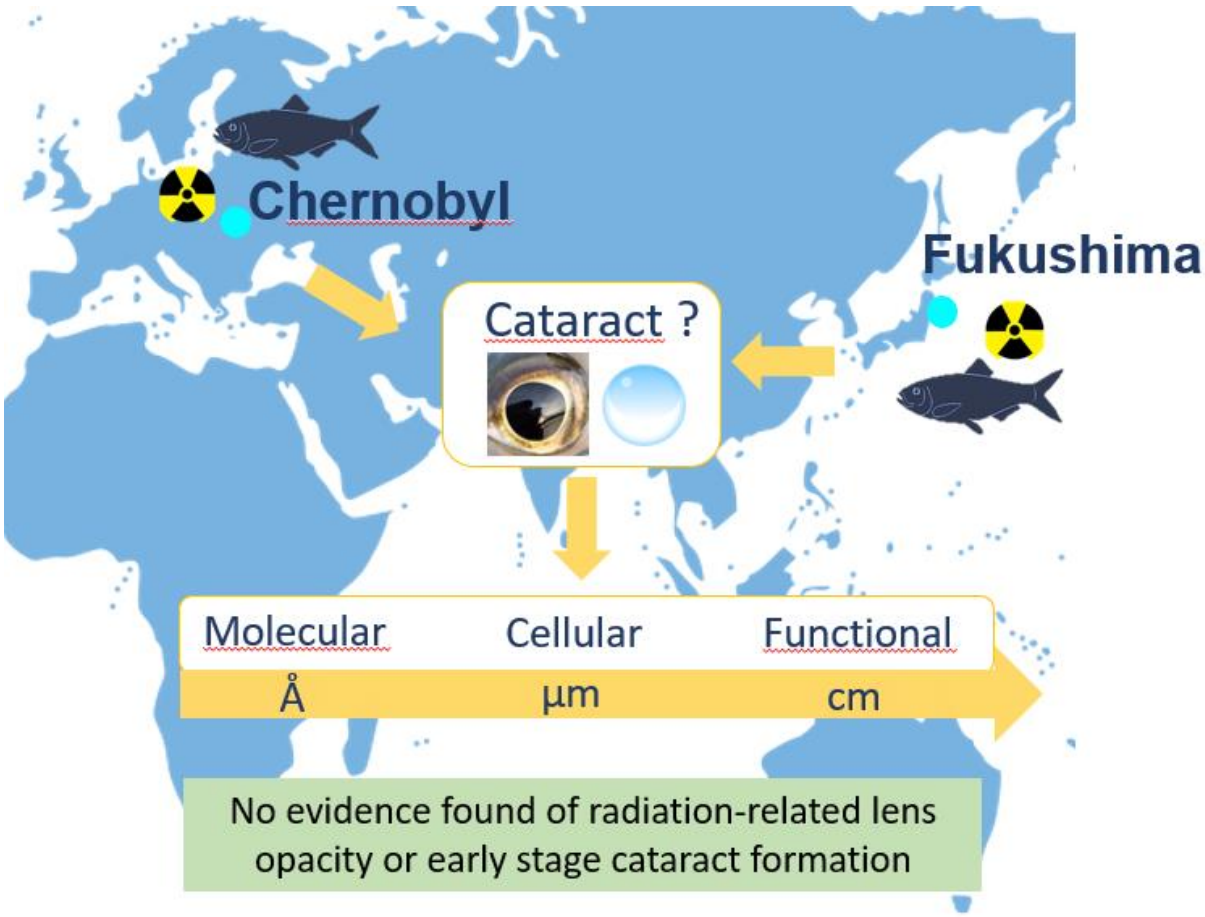

Abstract

Recent studies apparently finding deleterious effects of radiation exposure on cataract formation in birds and voles living near Chernobyl represent a major challenge to current radiation protection regulations. This study conducted an integrated assessment of radiation exposure on cataractogenesis using the most advanced technologies available to assess the cataract status of lenses extracted from fish caught at both Chernobyl in Ukraine and Fukushima in Japan. It was hypothesised that these novel data would reveal positive correlations between radiation dose and early indicators of cataract formation.

The structure, function and optical properties of lenses were analysed from atomic to millimetre length scales. We measured the short-range order of the lens crystallin proteins using Small Angle X-Ray Scattering (SAXS) at both the SPring-8 and DIAMOND synchrotrons, the profile of the graded refractive index generated by these proteins, the epithelial cell density and organisation and finally the focal length of each lens.

The results showed no evidence of a difference between the focal length, the epithelial cell densities, the refractive indices, the interference functions and the short-range order of crystallin proteins (X-ray diffraction patterns) in lens from fish exposed to different radiation doses. It could be argued that animals in the natural environment which developed cataract would be more likely, for example, to suffer predation leading to survivor bias. But the cross-length scale study presented here, by evaluating small scale molecular and cellular changes in the lens (pre-cataract formation) significantly mitigates against this issue.

Introduction

The formation of cataract in humans due to occupational or accidental exposure to acute ionising radiation is well documented (ICRP, 2012). Data on cataract incidence with long follow up periods of atomic bomb survivors, astronauts, residents of the Chernobyl nuclear exclusion zone and radiation workers have shown that radiation associated lens opacities occurred at much lower doses than previously thought (Bouffler et al., 2012). Consequently, the International Commission on Radiological Protection (ICRP) decreased the risk threshold of the absorbed dose from 2 to 0.5 Gy (ICRP, 2012), which is within the range of possible cumulative lifetime doses to which animals at Chernobyl and Fukushima could be exposed.

Little is known about the effect of long-term chronic exposure through the life span of organisms exposed to ionising radiation in the natural environment. In the laboratory, amphibians, rabbits, rodents and fish have all been used as models for the effects of radiation upon the eye and the lens (Worgul et al, 1976; Barnard et al, 2019; von Sallmann 1951; Geiger et al., 2006). Lens development is very highly conserved from teleost fish to man (Wu et al., 2015; Greiling et al., 2010; Cardozo et al., 2023; Morishita et al., 2021; Kamei and Duan, 2021; Wang et al., 2021). Studies in the natural environment have proved contradictory. While a significant increase in cataract incidence was claimed in birds and voles at Chernobyl (Mousseau and Møller, 2013; Lehmann et al., 2016) (the latter at cumulative doses lower than 1 mGy). A study at Fukushima at cumulative dose rates up to 1600 mGy did not, however, find any significant effects on cataract formation in wild boar (Pederson et al., 2020).

An in-vitro laboratory study (Kocemba and Waker, 2021) on rainbow trout lenses found no change in focal length variability at doses up to 2200 mGy (acute). Studies finding significant effects of radiation on cataract in wildlife at Chernobyl (Mousseau and Møller 2013, Lehmann et al., 2016) have generated significant media coverage and, if true, would represent a major challenge to current radiation protection regulation. The Lehman et al. (2016) study has, however, been criticised due to its subjective nature, poor sample preservation and the lack of evidence to support its conclusions (Smith 2020). Similarly, a study of cataracts in birds (Mousseau and Møller 2013) has been criticised for lack of ophthalmologic expertise in identifying cataract incidence (Pederson et al. 2020).

An opaque lens is highly disadvantageous for the survival of wild organisms as clear vision is required for hunting, feeding and to evade predation. Therefore, studies finding no effect of radiation on cataract incidence could select for individuals lacking cataracts or with compromised vision. Pre-cataract phenotypes can be identified by *in vivo* evaluation methods that measure the loss of lens transparency because of protein aggregation and epithelial cell density changes (Markiewicz et al., 2015; Barnard et al 2018; Vigneux et al 2022). Our study uses two different techniques to measure such changes which can indicate early-stage cataract formation and are therefore more sensitive and less subjective than previous evaluations which apparently observed radiation induced cataract in free-living organisms (Mousseau and Møller 2013; Lehmann et al., 2016). The first method we use measures cell densities using confocal light microscopy and image analysis software to create three-dimensional maps for the epithelium (Kalligeraki et al., 2020). The second method measures potential ultrastructural changes to the constituent crystallin proteins within the lens fibre cells using the low angle X-ray diffraction method. Changes in the structural conformation of lens crystallin proteins manifest themselves as protein aggregates leading then to an opacity. The degree of this opacity can be accurately and sensitively measured using small angle X-ray scatter (SAXS) (Regini et al., 2004; Regini and Meek, 2009).

Fish species are highly relevant to study ionising radiation effects since they reflect the health of the environment and can be used as surrogates in the assessment of the effects of stressors on human health (Sipes et al., 2011; Horzmann & Freeman, 2018; Pinna et al., 2023). Moreover, they are considered as the most radiosensitive aquatic species (Sazykina and Kryshev, 2003) and have been highly exposed in freshwater systems at Chernobyl and both freshwater and marine systems in Fukushima. At Chernobyl, the total dose absorbed in a year for perch and roach can reach 142 and 129 mGy respectively and a cumulative dose at the time of catch is, respectively, about 645 and 710 mGy over a 5-year life span. These levels are more than 100 times higher than the levels hypothesised to induce cataract in voles from Chernobyl (Lehmann et al., 2016) and higher than the ICRP recommended thresholds for human cataract risk. It should be noted, however, that (as discussed below) dose estimation to the lens of free-living organisms is highly uncertain.

For the first time, the methods applied here provide an objective and quantitative analysis of potential radiation influence of cataract formation in free-living organisms. Uniquely, fish lens

sample from both Chernobyl and Fukushima are analysed, allowing comparison of fish of different exposure and life histories. It was hypothesised that these novel data would reveal positive correlations between radiation dose and cataract formation.

Methods

Optimisation of lens cryopreservation

An experiment was performed to optimise the cryopreservation buffer composition suitable to preserve the structure of the fresh lens from collection in the field to the laboratory analyses. To our knowledge this is the first cryopreservation buffer composition optimised for lens preservation. Rainbow trout lenses were used to test the efficiency of 21 different cryopreservation buffers by using a teleost buffer (composed of 111 mM NaCl; 5.4 mM KCl; 1 mM $CaCl_2$; 0.6 mM $MgSO_4$ and 5 mM HEPES) and varying the concentration of sucrose (100 to 200 mM), glycerol (0 to 100%) and DMSO (0 to 100%) for optimal preservation of the lens. A total of 31 fish and their 62 lenses were used. Three replicates were used for each condition except for one in which two replicates were used. Samples were kept for a period of 8 days at - 196 °C in the dry shipper used for field samples collection. They were defrosted at 4°C for 24h.

The most intact lenses were assessed by observing transparency and any signs of opacity or structural changes using an optical microscope (Zeiss) together with statistical analyses (glm, binomial).

Field study

Field studies were carried out in seven lakes in Ukraine and Belarus and two ponds and a river in Japan (Figure 1). Studies on the genetic and physiological health of fish in seven lakes in Belarus and Ukraine with a long-term exposure history to a gradient of radiation dose have brought significant accompanying data to enable calculation of dose rate and quantification of potential confounding factors such as parasite loads, water chemistry (major cations, nitrates) environmental parameters (pH, T°C, dissolved oxygen) and other radioisotopes specific activity (Lerebours et al., 2018; 2020). Several studies in Japan in fish from water ponds and rivers from Fukushima prefecture characterised the Cs activity and distribution (Wakiyama et al., 2017; Wada et al., 2019) also enabling a robust dose rate calculation.

One lens of each of 103 perch (*Perca fluviatilis*) collected in spring 2016 at Chernobyl in seven lakes representing a gradient of radiation dose were analysed for refractive index, length radius and focal length measurements (Table S1). Perch from a control lake (Dvorische), outside the exclusion zone, and from a highly contaminated lake (Glubokoye), inside the exclusion zone, were analysed for refractive index and Bragg Spacing using the Spring 8 synchrotron and using the Diamond synchrotron (Table S2). An old (>12 years) carp (*Cyprinus carpio*) with visible cataract from the cooling pond was collected and analysed as a positive control. Carp (*Carassius auratus*) were also collected in ponds inside the exclusion zone in the Fukushima prefecture (Suzuuchia and Funazawa Ponds; Wakiyama et al., 2017) and outside the exclusion zone, in Abukuma river (Shinobu Dam; Mitamura et al., 2022) for SAXS analyses (Table S2).

The age was determined by counting the number of annuli on the scales (Chernobyl lakes) and otoliths (ponds from Fukushima prefecture). Age is given in SI Table S1, being in the range 4-5 years for Chernobyl fish and 6-7 years for fish at Fukushima.

Dose estimation

Internal and external dose was estimated from measurements of radioactivity in whole fish, fish lenses and sediments.

Lens samples were analysed at GAU-Radioanalytical were as follows: lenses were transferred to counting vials for analysis as received by gamma spectrometry. High-resolution gamma spectrometric analysis was performed using HPGe detectors. Detectors were calibrated against a mixed radionuclide standard solution. The standard was used to prepare a source of identical geometry to that of the samples. Gamma spectra were analysed and individual radionuclides quantified using Fitzpeaks spectral deconvolution software (JF Computing Services).

For radiochemical analysis, lens samples were spiked with ^{85}Sr, ^{232}U, ^{242}Pu and ^{243}Am tracers for chemical recovery monitoring.

Measurements of radioactivity in sediments at Fukushima were taken from Konoplev et al. (2018) and those in fish followed the radioanalytical method described in Wada et al. (2019) Measurements of radioactivity in sediments and fish at Chernobyl were taken from Lerebours et al. (2018). Internal and external doses were calculated using the ERICA tool (Brown et al. 2008).

Focal length and effective refractive index measurements

The effective focal length and (uniform) refractive index measurements were made using a previously published approach (Young et al., 2018) with a modified set up, as shown in Supplementary Information Figure S1. A custom 3D printed holder was used to suspend the sample lens in a diluted solution of fluorescein such that its optical axis was aligned vertically. A 488 nm fibre-coupled laser source (Stradus Versalase, Vortran) was mounted directly above the sample lens above a collimator. The incident illumination was focused by the sample lens into the fluorescein solution causing localised fluorescence excitation. The fluorescence emission was imaged through a glass viewing window and a spectral filter (MDF-GFP, Thorlabs) by a CCD (QI Click Mono, 01-QICLICK-R-F- M-12, QImaging) that was aligned horizontally on the bench. A brightfield image was also captured by removing the fluorescence filter. The pixel scale of the camera was calibrated by imaging a diffraction grating with two line pairs per mm and the line separation determined to be 10.4 pixels.

The optimum value for the refractive index was recorded and the effective focal length of the lens was calculated using the ball lens equation:

$$f = \frac{nR}{2(n-1)}$$

where n is ratio of the refractive index of the lens, nlens, to the refractive index of the surrounding medium (assumed to be water, nwater = 1.333) and R is the radius of the lens. The method and calibration were verified using a BK7 glass ball lens (04VQ06, Comar), which was found to have a refractive index of 1.526 ± 0.008. This was in good agreement with the refractive index of BK7 Schott glass at 488 nm, which is 1.522.

Hoechst Staining, cell density measurements of the lens epithelia

The measurement of the epithelial cell densities in lenses taken from fish caught in control and exposed lakes is as described (Kalligeraki et al., 2020). The globes had been fixed in 4% (w/v) PFA in phosphate buffered saline (PBS) and the lenses were removed from the globe prior to staining with 10µM Hoechst 33324 (Merck Life Sciences, UK) after permeabilising with 0.5% (w/v) Triton-X-100 in PBS for up to an hour at room temperature. The lenses were washed in PBS, then mounted on the acrylamide support and positioned prior to imaging using a Leica SP5 II confocal microscope equipped with an HXC APO × 10/0.40 NA oil (n = 1.518) immersion objective (Supplementary Information Figure S2). Data collection and analysis are as described (Kalligeraki et al., 2020), collecting data from the meridional rows of the lens epithelium where radiation damage has been reported in mouse models exposed to low dose ionising radiation (IR) (Markiewicz et al., 2015).

SPring-8 X-ray interferometric analyses

Fresh piscine lenses from four perch *P. fluviatilis*, two inside (Lake Glubokoye) and two outside (Lake Dvorische) the exclusion zone of Chernobyl and an old carp, *C. carpio*, from the Cooling Pond used as a positive control, were transported from UK to Japan for measurement of refractive index at the SPring-8 synchrotron. One lens was analysed from each of the fish from Dvorische and two lenses from each fish from Glubokoye. Samples were set in 2% agarose gel within a special cell for measurement on beamline BL20B2 using X-ray phase tomography based on X-ray Talbot interferometry (Hoshino et al., 2010; Hoshino et al., 2011; Momose, 2005). More detail on the Spring-8 methods can be found in Supplementary Information.

DIAMOND synchrotron analyses

Small angle X-ray scattering (SAXS) studies on the fish lenses collected from Chernobyl and Fukushima were also conducted at the Diamond Synchrotron (Didcot, Oxfordshire UK) on small angle beam line I22 (Smith et al., 2021). The lenses were placed in an airtight Perspex sample holder with Mylar windows which are X-ray transparent. Each sample holder was secured on to a motorised stage which could be moved horizontally and vertically in respect to the X-ray beam. The X-ray diffraction patterns were collected separately from each lens. The X-ray camera was 6.25 metres in length. The data were collected using an X-ray beam size 80µm x 250µm, with a wavelength of 1Å, directed perpendicularly to the whole lens for a 2D

grid scan of each lens. The exposure time for each individual X-ray diffraction pattern was 0.1 sec at 0.5 mm intervals along the lens horizontal and vertical meridians. Individual X-ray diffraction patterns were recorded using a Pilatus P3-2M(SAXS) detector. Each 2D grid scan varied in size length in both the x and y directions depending on the size of each individual lens. After the data were processed and the background subtracted from each individual X-ray pattern, a montage of all X-ray patterns for each lens was created separately using Diamond's in house DAWN 2.11.0 software package (Basham et al., 2015; Filik et al., 2017).

Statistical analyses

All statistical tests were performed using R Studio (v4.0.1). Any potential difference in the refractive index, lens radius and focal length was assessed by performing a t-test. The efficiency of the different buffers on the structural appearance of the lenses after a freezing period of 8 days was assessed by using a generalised linear model (glm) and using a binomial family.

Results

Cryopreservation optimisation

The cryopreservation buffer showing the best result ($p < 0.05$) was composed of the teleost buffer and 200 mM of sucrose, 60% (v/v) of glycerol and 40% (v/v) DMSO and was thus used to preserve field samples.

Dose estimation

Fish lens samples were analysed for ^{60}Co, ^{90}Sr, ^{137}Cs, ^{241}Am and isotopes of Pu as well as a range of natural radionuclides. All artificial radionuclides were below l.o.d. except for ^{137}Cs which ranged from 0.08 Bq/g (f.w.) in lake Suuzuchi to 0.32 Bq/g (f.w.) in lake Glubokoye. All natural radionuclides were below l.o.d. except for ^{40}K which was 0.56 Bq/g (f.w.) in Funazawa and 0.64 Bq/g (f.w.) in the Chernobyl Cooling Reservoir, all others being below l.o.d.

As expected, uptake of artificial radionuclides to the lens was very low, so dose to the lens from radioactivity within the lens is negligible compared to that from the fish body and bed sediment. It was therefore appropriate to estimate dose to the lens from the combination of internal dose from ^{134,137}Cs in the fish body and external dose from sediment. The ERICA

software was used to estimate internal and external dose based on measured fish and sediment activity concentration. Sediment activity concentration from the lakes in Japan were obtained from Konoplev et al., (2018). It was assumed that each fish spent 50% if its time near to the sediment and 50% in open water.

Estimated doses to the lens are given in Table 1. External dose rates are estimated to be significantly greater than internal in the Japanese lakes, but are of the same order as internal in the three most contaminated Ukrainian lakes due to the significance of ^{90}Sr beta dose within the CEZ. Uncertainty in external dose estimates is driven primarily by the assumed occupancy factor (the amount of time the fish is close to bed sediments). Given this and other uncertainties, estimated dose rates should be treated as relative rather than absolute. Natural background radiation doses to aquatic organisms hve been estimated to be in the range 0.022-0.18 μGy h^{-1} (Garnier-Laplace et al., 2006) though could be significantly higher in high natural background radiation areas. In the Chernobyl Cooling Pond, Kryshev and Sazykina (1995) estimated natural radiation dose rates to be approximately 0.04-0.08 μGy h^{-1}.

Cell density and optical properties

Optical properties of the lenses taken from fish from seven different lakes across a gradient of contamination at Chernobyl are summarised in Supplementary Information Table S3. No significant differences were seen between the optical properties of the lenses taken from fish caught from different lakes at Chernobyl (Figure 2).

Nucleus density measured in 20 lenses from one low contamination lake (Dvorische) and one high contamination lake (Glubokoye) showed no significant differences between lakes (Figure 3 see also SI Figures S3; S4 for data from other lakes). Variance increased in areas of higher density, whereas areas of lower density showed higher order in both lakes. To demonstrate variance within samples, we have included standard deviation on error bars in Figure 3.

Spring-8 Refractive Index analysis

High resolution refractive index analysis at Spring-8 showed no evidence of a difference in refractive index between the relatively uncontaminated Lake Dvorische and the most contaminated lake in this study, Lake Glubokoye (Figure 4).

A montage from a Spring-8 2D grid scan from a Crucian Carp lens collected from the Shinobu dam of the Abukuma river, Fukushima, is shown in Supplementary Information Figure S5. Each individual X-ray pattern from the lens in the montage is dominated by a single X-ray reflection which is a broad diffuse ring. The putative interpretation of this reflection is that it is an interference function, and originates from the average nearest neighbour spacing between the crystallin proteins. This measurement is known as the Bragg spacing (d). The width or thickness of this reflection gives an indication of crystallin proteins ordering within the lens fibre cells, with a narrower interference function indicating a high degree of ordering (Regini et al, 2004, Regini and Meek, 2009).

The inference function spacings from a lens taken from Suzuuchi Pond (approx. dose rate 5.5 μGy h^{-1}) were calculated. From each montage, a column of individual X-ray diffraction patterns was chosen next to the vertical meridian of the lens. A circular integration was performed on each pattern and the resulting X-ray intensity (I) profiles plotted as a function of inverse space (Q). Figure 5 shows a typical intensity profile from a Suzuuchi Crucian Carp lens with the peak of the interference clearly visible.

Figure 6 shows a plot of the Bragg spacings from the central meridians of the 2D grid scans of Crucian Carp lenses from Glubokoye lake and the relatively uncontaminaded Lake Dvorische as a function of distance across the lens. As can be seen in both lenses, the Bragg spacing decreases from one periphery of the lens towards to centre, and then increases again to the opposite periphery. This is expected due to increase in crystallin protein concentration, and hence a decrease in the average nearest neighbour spacing between the crystallin proteins. The change in the protein concentration is directly responsible for the refractive index gradient found in many different types of animal lenses (Pierscionek and Regini, 2012). There is an asymmetry in the spacing trends in both lenses towards the edge of each lens. This may be due to the individual differences in refractive index gradients of the lenses at the edges (see Figure 6), which in turn would lead to a localised variation in the Bragg spacings. Overall, the spacings between the two lenses is remarkably similar and only vary by a maximum of 10 Å. If there had been a large amount of insoluble large amorphous aggregates leading to cataract formation in one of the lenses, we would expect to see a much larger change in the spacings between the two accompanied by a dramatic widening of the profile of the interference function as observed

by Suárez et al. (1993). Therefore, the data indicate that there are no appreciable structural differences at this length scale between the Crucian Carp lenses from the contaminated (Glubokoye) compared to uncontaminated (Dvorische) lake.

As a positive control, we performed a DIAMOND 2D grid scan on a Chernobyl Carp lens with a dense nuclear cataract which was clearly visible. The density and location of this opacity suggests that it is age-related and not caused by radiation. The oldest cells in the lens are found in its centre (lens nucleus) and these are more prone to age-related cataract formation (Quinlan and Clark, 2022). It was found that in the vast majority of the individual X-ray diffraction patterns from the lens that the interference function was not present. We attribute this to the formation of many large insoluble amorphous aggregates. Some extremely diffuse interference functions were observed in some individual X-ray diffraction patterns at the edges of the lens, away from the nucleus. Figure 5 (b) shows the Log X-ray intensity profile of a such a pattern. As can be seen, the interference function has become so broad that it has almost disappeared, it is also much closer to the centre of the pattern when compared to that in Figure 5 (a) i.e. a larger Bragg spacing.

Discussion

This study spans the length scales from mm to sub-nm resolution by measuring the optical properties, refractive index profiles, epithelial cell densities and X-ray synchrotron analysis of molecular aggregation and cataract formation. We found no evidence of a significant impact of radiation on lens development, protein and cell organisation and optical function in fish sampled from waterbodies at Chernobyl and Fukushima. The total dose absorbed in a year for perch and roach in Chernobyl lakes reached 142 and 129 mGy respectively with a cumulative dose at the time of catch of 645 and 710 mGy respectively over a 5-year life span. These levels are more than 100 times higher than the doses previously hypothesised to induce cataract in voles from Chernobyl (Lehmann et al., 2016). Our study agrees with more recent findings reported for animals at Fukushima where wild boar were exposed to cumulative doses up to 1600 mGy without any significant signs of cataract formation (Pederson et al., 2020).

Exposure to high acute dose or chronic low dose IR can result in measurable changes in lens structure and function (see Uwineza et al., 2019 for a recent review). For example,

accumulative doses of 0.5, 1 and 2 Gy for different dose rates of 0.063 Gy/min and 0.3 Gy/min increased epithelial cell division (Barnard et al., 2022; Markiewicz et.al., 2015) altered epithelial cell density and disorganisation of the epithelial cells in the transitional zone and meridional rows at the most distal edge of the epithelium (Markiewicz et. al., 2015). Long-term consequences of such exposures can be altered lens shape (Markiewicz et. al., 2015) and lens opacification (Barnard et. al., 2022) depending on the radiosensitivity of the mouse strain used. When the loss of visual acuity was monitored by Optical Coherence Tomography (OCT), then posterior subcapsular cataracts were the most prevalent cataract type observed (Pawliczek et.al., 2022), even after a single acute dose of 0.5 Gy (Kunze et. al., 2021).

For humans, the Lifespan Study of atomic bomb survivors and other studies showed that the eye lens is a particularly radiosensitive tissue with a long latency observed between exposure and the appearance of vision-impairing cataract (Hamada et al., 2020). This has called into the question the concept of a defined threshold dose (Hamada et.al., 2020). The United States National Council on Radiation Protection and Measurements (NCRP) has not assigned a specific threshold dose because of the limitations associated with available epidemiological studies (NCRP 2016), demonstrating the importance of gathering data from all sources to determine whether cataract is either a tissue reaction or a stochastic effect or a mixture of both by the lens (Hamada et. al., 2020).

We did not find a significant difference in density of lens epithelial cells between fish from waterbodies of different levels of ionising radiation. The density and organisation of the meridional rows of lens epithelial cells at the very periphery of the lens epithelium is altered by aging Wu et al., 2015, by diet (Gona, 1984) and by exposure to radiation, both ionising (Zintz and Beebe, 1986, Pendergrass et al., 2010, Markiewicz et al., 2015) and non-ionising radiation Wei, Hao et al. 2021). Zebrafish are an established radiobiological model (Geiger, Parker et al. 2006, Liu et al., 2020, Marques et al., 2020) and the developing eye and fish lens is a key sensor of both toxic (Sipes et al., 2011) and radioprotective agents (Liu et al., 2020). In early zebrafish development, a total IR exposure of 1.62mGy was sufficient to differentially regulate genes that would be expected to have lens effects as they are transcription factors expressed during and following lens development (trp53, TGFb1, cebpa, crabp2 and vegfa; https://research.bioinformatics.udel.edu/iSyTE/). A dose of 0.4 mGy/hr continuous for 92

hours produced developmental deformities which included head and eye deformities (Hurem et al., 2017). For non-ionising radiation, early studies had indicated the sensitivity of teleost, mouse, rabbit and human to UVB (290-320nm) was similar (Cullen and Montieth-McMaster 1993; Cullen et al 1994).The chronic exposure of trout to levels of UVB radiation equivalent to the daily accumulative dose of 500J/cm^2 over a 205 day period demonstrated the formation of anterior opacities detected by slit-lamp analyses (Cullen et al., 1994). This study also suggested that the age of the fish could influence cataract incidence (Cullen et al; 1994) and that UVB exposure could accelerate the aging process (Zigman, 1983). Exposure to ionising radiation is also believed to accelerate age-related cataract (Uwineza et al., 2019). In later studies, the near to threshold UVB dose for rats (Michael and Brismar, 2001; Galichanin et al 2010; Hurem et al 2017) produced changes in the refractive index gradient (Michel and Bismar 2001) that were irreversible (Galichanin et al., 2008). It seems reasonable therefore to expect the eyes and lenses of teleosts to be similar to other animal models.

In the perch fish taken from the lakes around Chernobyl, no statistically significant changes in the distribution and density of the lens epithelial cells in the and adjacent to the meridional rows in the epithelium were observed. We know that dose (Markiewicz, Barnard et al. 2015)) and dose rate (Barnard et al., 2019, Barnard et al., 2022) affect the mouse lens response to ionising radiation. The response to low dose ionising radiation by human lenses (Della Vecchia et al., 2020; Little et al., 2021; Su et al., 2021) can be associated with increased cataract incidence. There is evidence the doses and dose rates experienced by voles in the Chernobyl area would be sufficient to cause opacities and cataract (Kleiman et al., 2017), though methods and interpretation are not presented in the Kleiman et al. (2017) summary abstract. Lens opacities affect species fitness (Flink et al., 2017), responses to predators (Flink et al., 2017) and diet selection (Vivas Muñoz et al., 2021), but the perch examined in the different Chernobyl locations showed no statistically significant differences in their lens metrics or optical properties.

A previous SAXS study of human lenses (Suárez et al., 1993) found that the inference function becomes much broader and the spacing increases greatly with the age of the lenses, especially past the age of 55 years in humans. These authors found that Bragg spacing (which arises from the average centre to centre distance between the crystallin proteins) from a single X-ray pattern

from the centre of each lens increased from 142Å from a very young lens to 200Å in a lens with more insoluble protein and increasing light scatter has aging events that eventually lead to lens opacification (reviewed in Quinlan and Clark, 2022). The dramatic changes in the interference function are explained in terms of the structural conversion of the crystallin proteins with age (Regini and Meek, 2009). These proteins become denatured in response to environmental stresses such as radiation, temperature, glycation and oxidation. The denatured proteins are thought to combine to form water insoluble amorphous aggregates. As these amorphous aggregates grow, they increase the average nearest neighbour spacing between the crystallin proteins and detrimentally affect the order of proteins and water which is integral to maintaining transparency. When the amorphous aggregates become comparable in size to the wavelengths of the visible spectrum, they scatter light causing lens opacities. If the cataract is very dense, the average nearest neighbour spacing between the crystallin proteins becomes so large that the inference function disappears from the X-ray diffraction pattern (Figure 5b). This isolated case is most likely to be related to the age of the fish (>12 years), given its position in the central and oldest part of the lens.

We would expect that lenses which have been exposed to ionising radiation of a sufficient dose would have increased levels of insoluble proteins in the form of amorphous aggregates, even before opacities in the lens become visible as conceptualised in the cataractogenic load hypothesis (Uwineza et.al., 2019; Quinlan and Cark, 2022). This would result in a large increase in the Bragg spacing of around 60 Å. As Figure 6 illustrates, such a large increase was not evident in any of the lenses (15 lenses studied) of fish from Chernobyl and Fukushima, except the sample from the old (>12 years) Crucian Carp with a visible central cataract. Of course, it was only feasible to study a proportion of the fish population by synchrotron methods. We cannot rule out the existence of cataract or pre-cataract in fish which were not studied. Nevertheless, the synchrotron method is the most sensitive available to detect altered protein-protein associations and protein aggregation as indicators of any pre-cataract or cataract phenotype. For 15 lenses studied by synchrotron, 40 lenses (from contaminated lakes) studied for refractive index and 20 (from contaminated lakes) for epithelial cell density, this was not the case, suggesting that this the likely situation for the wider fish population.

It is further noted that we cannot completely exclude radiation-induced cataractogenesis in the fish populations of these lakes. Other potential indicators of cataract formation (including biochemical differences such as oxidative stress) were not studied. Further, it was only possible to gain a representative sample of similar age (4-5 years) fish from each of the lakes. Older fish may provide better evidence of radiation induced cataract but it was not feasible to obtain a large and age consistent sample of old fish due to their relatively much lower numbers in the population.It should also be noted that in all studies of wild animals, particularly aquatic organisms, dose rate estimation is highly uncertain owing to changes in exposure during the development and lifetime of the organism and to uncertainty of movement and habitat. Thus the estimated doses calculated here should be treated with caution, though relative doses between groups of fish from different sites are much more accurate since development and habitat occupancy factors are similar between sites. Further laboratory experiments which can better control dose and dose rate (albeit with the limitation of relatively short duration) would be valuable to complement studies in the natural environment.

It could also be argued that animals in the natural environment that developed cataract would be more likely to be predated leading to survivor bias, but the small scale molecular and cellular changes we have studied (ie pre-cataract formation) would mitigate against this.

Uncertainty in dose rate estimation could explain some differences in findings about cataract formation in wild animals. However, because relative doses between waterbodies are much more accurate than absolute doses, they are not sufficient to explain the difference between our findings and those of Lehman et al. (2016) (voles) and Mousseau and Moller (2013) (birds) studies. These latter findings of cataract formation at very low doses and dose rates are in contradiction to ICRP guidance based on laboratory animal and human epidemiological data. They are further not supported by the field study findings reported here for fish and previously for wild boar Pederson et al. (2020)). It has been suggested that the earlier studies (Lehman et al. 2016; Mousseau et al. 2013) had significant methodological and interpretation issues (Smith et al. 2017, Pederson et al. 2020).

There may be differences in lens development and structure between species which could affect the formation of radiation-induced cataract. Lens development across vertebrates is very well

conserved as discussed in the Introduction. The development and structure of fish lenses are similar in terms of their protein content, type of proteins and in the protein distribution across the lens which creates the refractive index (Sivak 2004; Kocemba and Waker, 2021). Hence, any response to factors that cause cataract will be broadly similar. However, whilst both fish and rodent lenses are abundant in γ-crystallin, the latter contain γS-crystallin, but the former are rich in γM-crystallin (Mahler et al, 2013). The low tryptophan and high methionine content in γM-crystallin may offer a protective effect given that methionine has been shown to provide radiation protection (Vuyyuri et al, 2008; Mahler et al 2013).

The present study has observed no radiation induced cataract or evidence of pre-cataract lens damage in wild fish exposed to relatively high cumulative dose (but relatively low dose rate) radiation. As the lens grows, each layer of lens fibres laid down by the differentiated epithelial cells is a 'snap shot' or 'time capsule' of its history recorded for posterity in a similar manner to tree rings. Consequently, the lens represents both an endpoint of exposure history and a timeline of accumulated damage which is highly relevant under chronic exposure scenarios.

Acknowledgments. Authors are grateful to L. Nagorskaya, D. Gudkov, V. Rizewski, A. Kaglyan, A. Zubey, A. Leshchenko, and N. Fuller. This work was part funded by the TREE (Transfer-Exposure-Effects) consortium under the RATE programme (Radioactivity and the Environment), funded by the Environment Agency and Radioactive Waste Management Ltd (NERC grant NE/L000393/1), by the STFC ENV-RAD-NET Small Research Fund and Diamond Light Source for beamtime (proposal SM17075). Award for beam time from SPring-8 is gratefully acknowledged (proposal number 2015A1864). RAQ and AU were part of the LDLensRad project that received funding from the Euratom research and training programme 2014-2018 in the framework of the CONCERT [Grant agreement No 662287]. This publication reflects only the author's view. Responsibility for the information and views expressed therein lies entirely with the authors. The financial support of the National Eye Research Foundation (AAK; SAC014), Fight for Sight (RAQ; 1584/85), Leverhulme Trust (RAQ; RPG-2012-554) and EPSRC (JMG, LY; EP/M010767/1, EPI010173/1) are gratefully acknowledged.

References

Barnard S, Moquet J, Lloyd S, Ellender M, Ainsbury E, Quinlan R. Dotting the eyes: mouse strain dependency of the lens epithelium to low dose radiation-induced DNA damage. International Journal of Radiation Biology 2018; 94: 1116-1124.

Barnard S, Uwineza A, Kalligeraki A, McCarron R, Kruse F, Ainsbury E, et al. Lens epithelial cell proliferation in response to ionizing radiation. Radiation research 2022; 197: 92-99.

Barnard SG, McCarron R, Moquet J, Quinlan R, Ainsbury E. Inverse dose-rate effect of ionising radiation on residual 53BP1 foci in the eye lens. Scientific reports 2019; 9: 10418.

Basham M, Filik J, Wharmby MT, Chang PC, El Kassaby B, Gerring M, et al. Data analysis workbench (DAWN). Journal of synchrotron radiation 2015; 22: 853-858.

Bouffler S, Ainsbury E, Gilvin P, Harrison J. Radiation-induced cataracts: the Health Protection Agency's response to the ICRP statement on tissue reactions and recommendation on the dose limit for the eye lens. Journal of Radiological Protection 2012; 32: 479.

Brown J, Alfonso B, Avila R, Beresford NA, Copplestone D, Pröhl G, et al. The ERICA tool. Journal of Environmental Radioactivity 2008; 99: 1371-1383.

Cardozo MJ, Sánchez-Bustamante E, Bovolenta P. Optic cup morphogenesis across species and related inborn human eye defects. Development 2023; 150: dev200399.

Cullen A, Monteith-McMaster C. Damage to the rainbow trout (Oncorhyncus mykiss) lens following an acute dose of UVB. Current Eye Research 1993; 12: 97-106.

Dauer LT, Ainsbury EA, Dynlacht J, Hoel D, Klein BE, Mayer D, et al. Guidance on radiation dose limits for the lens of the eye: overview of the recommendations in NCRP Commentary No. 26. International journal of radiation biology 2017; 93: 1015-1023.

Della Vecchia E, Modenese A, Loney T, Muscatello M, Paulo MS, Rossi G, et al. Risk of cataract in health care workers exposed to ionizing radiation: a systematic review. La Medicina del lavoro 2020; 111: 269.

Filik J, Ashton A, Chang P, Chater P, Day S, Drakopoulos M, et al. Processing two-dimensional X-ray diffraction and small-angle scattering data in DAWN 2. Journal of applied crystallography 2017; 50: 959-966.

Flink H, Behrens JW, Svensson PA. Consequences of eye fluke infection on anti-predator behaviours in invasive round gobies in Kalmar Sound. Parasitology Research 2017; 116: 1653-1663.

GALICHANIN K, LI Y, MEYER L, LÖFGREN S, SÖDERBERG P. The lens response to daily in vivo exposures to UVR. Acta Ophthalmologica 2008; 86.

Garnier-Laplace J, Della-Vedova C, Gilbin R, Copplestone D, Hingston J, Ciffroy P. First derivation of predicted-no-effect values for freshwater and terrestrial ecosystems exposed to radioactive substances. Environmental science & technology 2006; 40: 6498-6505.

Geiger GA, Parker SE, Beothy AP, Tucker JA, Mullins MC, Kao GD. Zebrafish as a "biosensor"? Effects of ionizing radiation and amifostine on embryonic viability and development. Cancer research 2006; 66: 8172-8181.

Gona O. Cytoarchitectural changes in lens epithelium of galactose-fed rats. Experimental eye research 1984; 38: 647-652.

Greiling TM, Aose M, Clark JI. Cell fate and differentiation of the developing ocular lens. Investigative ophthalmology & visual science 2010; 51: 1540-1546.

Hamada N, Azizova TV, Little MP. An update on effects of ionizing radiation exposure on the eye. The British journal of radiology 2020; 93: 20190829.

Horzmann KA, Freeman JL. Making waves: New developments in toxicology with the zebrafish. Toxicological Sciences 2018; 163: 5-12.

Hoshino M, Uesugi K, Yagi N, Mohri S. Investigation of Imaging Properties of Mouse Eyes Using X-ray Phase Contrast Tomography. AIP Conference Proceedings. 1266. American Institute of Physics, 2010, pp. 57-61.

Hoshino M, Uesugi K, Yagi N, Mohri S, Regini J, Pierscionek B. Optical properties of in situ eye lenses measured with X-ray Talbot interferometry: a novel measure of growth processes. PLoS One 2011; 6: e25140.

ICRP. Statement on Tissue Reactions/Early and Late Effects of Radiation in Normal Tissues and Organs, Threshold Doses for Tissue Reactions in a Radiation Protection Context. ICRP publication 2012; 118: 40.

Kalligeraki AA, Isted A, Jarrin M, Uwineza A, Pal R, Saunter CD, et al. Three-dimensional data capture and analysis of intact eye lenses evidences emmetropia-associated changes in epithelial cell organization. Scientific reports 2020; 10: 16898.

Kamei H, Duan C. Alteration of organ size and allometric scaling by organ-specific targeting of IGF signaling. General and Comparative Endocrinology 2021; 314: 113922.

Kleiman NJ, Lavrinienko A, Kivisaari K, Boratynski Z, Dauer L, Mappes T, et al. Radiation Cataract in Chernobyl Voles. Investigative Ophthalmology & Visual Science 2017; 58: 2037-2037.

Kocemba M, Waker A. An investigation of early radiation damage in rainbow trout eye-lenses. Radiation and Environmental Biophysics 2021; 60: 421-430.

Konoplev A, Wakiyama Y, Wada T, Golosov V, Nanba K, Takase T. Radiocesium in ponds in the near zone of Fukushima Dai-ichi NPP. Water Resources 2018; 45: 589-597.

Kryshev I, Sazykina T. Assessment of radiation doses to aquatic organism's in the Chernobyl contaminated area. Journal of Environmental Radioactivity 1995; 28: 91-103.

Kunze S, Cecil A, Prehn C, Möller G, Ohlmann A, Wildner G, et al. Posterior subcapsular cataracts are a late effect after acute exposure to 0.5 Gy ionizing radiation in mice. International Journal of Radiation Biology 2021; 97: 529-540.

Lehmann P, Boratyński Z, Mappes T, Mousseau TA, Møller AP. Fitness costs of increased cataract frequency and cumulative radiation dose in natural mammalian populations from Chernobyl. Scientific Reports 2016; 6: 1-7.

Lerebours A, Gudkov D, Nagorskaya L, Kaglyan A, Rizewski V, Leshchenko A, et al. Impact of environmental radiation on the health and reproductive status of fish from Chernobyl. Environmental science & technology 2018; 52: 9442-9450.

Lerebours A, Robson S, Sharpe C, Nagorskaya L, Gudkov D, Haynes-Lovatt C, et al. Transcriptional changes in the ovaries of perch from Chernobyl. Environmental Science & Technology 2020; 54: 10078-10087.

Little MP, Azizova TV, Hamada N. Low-and moderate-dose non-cancer effects of ionizing radiation in directly exposed individuals, especially circulatory and ocular diseases: a review of the epidemiology. International Journal of Radiation Biology 2021; 97: 782-803.

Liu G, Zeng Y, Lv T, Mao T, Wei Y, Jia S, et al. High-throughput preparation of radioprotective polymers via Hantzsch's reaction for in vivo X-ray damage determination. Nature Communications 2020; 11: 6214.

Mahler B, Chen Y, Ford J, Thiel C, Wistow G, Wu Z. Structure and dynamics of the fish eye lens protein, γM7-crystallin. Biochemistry 2013; 52: 3579-3587.

Markiewicz E, Barnard S, Haines J, Coster M, Van Geel O, Wu W, et al. Nonlinear ionizing radiation-induced changes in eye lens cell proliferation, cyclin D1 expression and lens shape. Open biology 2015; 5: 150011.

Marques FG, Carvalho L, Sousa JS, Rino J, Diegues I, Poli E, et al. Low doses of ionizing radiation enhance angiogenesis and consequently accelerate post-embryonic development but not regeneration in zebrafish. Scientific Reports 2020; 10: 3137.

Meyer AJ, May MJ, Fricker M. Quantitative in vivo measurement of glutathione in Arabidopsis cells. The Plant Journal 2001; 27: 67-78.

Michael R, Brismar H. Lens growth and protein density in the rat lens after in vivo exposure to ultraviolet radiation. Investigative ophthalmology & visual science 2001; 42: 402-408.

Mitamura H, Wada T, Takagi J, Noda T, Hori T, Takasaki K, et al. Acoustic zone monitoring to quantify fine-scale movements of aquatic animals in a narrow water body. Environmental Biology of Fishes 2022; 105: 1919-1931.

Modarai B, Haulon S, Ainsbury E, Böckler D, Vano-Carruana E, Dawson J, et al. Editor's Choice–European Society for Vascular Surgery (ESVS) 2023 Clinical Practice Guidelines on Radiation Safety. European journal of vascular and endovascular surgery 2023; 65: 171-222.

Momose A. Recent advances in X-ray phase imaging. Japanese journal of applied physics 2005; 44: 6355.

Morishita H, Eguchi T, Tsukamoto S, Sakamaki Y, Takahashi S, Saito C, et al. Organelle degradation in the lens by PLAAT phospholipases. Nature 2021; 592: 634-638.

582 Mousseau TA, Møller AP. Elevated frequency of cataracts in birds from Chernobyl. PLoS One 2013; 8: e66939.
583 Padilla S, Corum D, Padnos B, Hunter D, Beam A, Houck K, et al. Zebrafish developmental screening of the
584 ToxCast™ Phase I chemical library. Reproductive toxicology 2012; 33: 174-187.
585 Pawliczek D, Fuchs H, Gailus-Durner V, de Angelis MH, Quinlan R, Graw J, et al. On the nature of murine radiation-
586 induced subcapsular cataracts: optical coherence tomography-based fine classification, in vivo dynamics
587 and impact on visual acuity. Radiation Research 2022; 197: 7-21.
588 Pederson SL, Li Puma MC, Hayes JM, Okuda K, Reilly CM, Beasley JC, et al. Effects of chronic low-dose radiation
589 on cataract prevalence and characterization in wild boar (Sus scrofa) from Fukushima, Japan. Scientific
590 reports 2020; 10: 1-14.
591 Pendergrass W, Zitnik G, Tsai R, Wolf N. X-ray induced cataract is preceded by LEC loss, and coincident with
592 accumulation of cortical DNA, and ROS; similarities with age-related cataracts. Molecular Vision 2010; 16:
593 1496.
594 Pierscionek BK, Regini JW. The gradient index lens of the eye: an opto-biological synchrony. Progress in retinal
595 and eye research 2012; 31: 332-349.
596 Pinna M, Zangaro F, Saccomanno B, Scalone C, Bozzeda F, Fanini L, et al. An Overview of Ecological Indicators of
597 Fish to Evaluate the Anthropogenic Pressures in Aquatic Ecosystems: From Traditional to Innovative DNA-
598 Based Approaches. Water 2023; 15: 949.
599 Quinlan RA, Clark JI. Insights into the biochemical and biophysical mechanisms mediating the longevity of the
600 transparent optics of the eye lens. Journal of Biological Chemistry 2022: 102537.
601 Regini JW, Grossmann JG, Burgio M, Malik N, Koretz J, Hodson SA, et al. Structural changes in α-crystallin and
602 whole eye lens during heating, observed by low-angle X-ray diffraction. Journal of molecular biology 2004;
603 336: 1185-1194.
604 Regini JW, Meek KM. Changes in the X-ray diffraction pattern from lens during a solid-to-liquid phase transition.
605 Current Eye Research 2009; 34: 492-500.
606 Sazykina T, Kryshev A. EPIC database on the effects of chronic radiation in fish: Russian/FSU data. Journal of
607 Environmental Radioactivity 2003; 68: 65-87.
608 Sipes NS, Padilla S, Knudsen TB. Zebrafish—As an integrative model for twenty-first century toxicity testing. Birth
609 Defects Research Part C: Embryo Today: Reviews 2011; 93: 256-267.
610 Sivak JG. Through the lens clearly: phylogeny and development: the Proctor lecture. Investigative
611 Ophthalmology & Visual Science 2004; 45: 740-747.
612 Smith A, Alcock S, Davidson L, Emmins J, Hiller Bardsley J, Holloway P, et al. I22: SAXS/WAXS beamline at
613 Diamond Light Source–an overview of 10 years operation. Journal of synchrotron radiation 2021; 28: 939-
614 947.
615 Smith J. Field evidence of significant effects of radiation on wildlife at chronic low dose rates is weak and often
616 misleading. A comment on “Is non-human species radiosensitivity in the 2 lab a good indicator of that in
617 the field? Making the comparison more robust” by 3 Beaugelin-Seiller et al. 4. 2020.
618 Su Y, Wang Y, Yoshinaga S, Zhu W, Tokonami S, Zou J, et al. Lens opacity prevalence among the residents in high
619 natural background radiation area in Yangjiang, China. Journal of Radiation Research 2021; 62: 67-72.
620 Suarez G, Oronsky A, Koch M. Age-dependent structural changes in intact human lenses detected by synchrotron
621 radiation X-ray scattering. Correlation with Maillard reaction protein fluorescence. Journal of Biological
622 Chemistry 1993; 268: 17716-17721.
623 Uwineza A, Kalligeraki AA, Hamada N, Jarrin M, Quinlan RA. Cataractogenic load–A concept to study the
624 contribution of ionizing radiation to accelerated aging in the eye lens. Mutation Research/Reviews in
625 Mutation Research 2019; 779: 68-81.
626 Vigneux G, Pirkkanen J, Laframboise T, Prescott H, Tharmalingam S, Thome C. Radiation-induced alterations in
627 proliferation, migration, and adhesion in lens epithelial cells and implications for cataract development.
628 Bioengineering 2022; 9: 29.
629 Vivas Muñoz JC, Feld CK, Hilt S, Manfrin A, Nachev M, Köster D, et al. Eye fluke infection changes diet composition
630 in juvenile European perch (Perca fluviatilis). Scientific reports 2021; 11: 3440.
631 VON SALLMANN L. Experimental studies on early lens changes after roentgen irradiation: I. Morphological and
632 cytochemical changes. AMA Archives of Ophthalmology 1951; 45: 149-164.

Von Sallmann L, Halver JE, Collins E, Grimes P. Thioacetamide-induced cataract with invasive proliferation of the lens epithelium in rainbow trout. Cancer research 1966; 26: 1819-1825.

Vuyyuri SB, Hamstra DA, Khanna D, Hamilton CA, Markwart SM, Campbell KC, et al. Evaluation of D-methionine as a novel oral radiation protector for prevention of mucositis. Clinical Cancer Research 2008; 14: 2161-2170.

Wada T, Konoplev A, Wakiyama Y, Watanabe K, Furuta Y, Morishita D, et al. Strong contrast of cesium radioactivity between marine and freshwater fish in Fukushima. Journal of Environmental Radioactivity 2019; 204: 132-142.

Wakiyama Y, Konoplev A, Wada T, Takase T, Byrnes I, Carradine M, et al. Behavior of 137Cs in ponds in the vicinity of the Fukushima Dai-ichi nuclear power plant. Journal of environmental radioactivity 2017; 178: 367-376.

Wang K, Vorontsova I, Hoshino M, Uesugi K, Yagi N, Hall JE, et al. Aquaporins have regional functions in development of refractive index in the zebrafish eye lens. Investigative Ophthalmology & Visual Science 2021; 62: 23-23.

Worgul BV, Merriam GR, Szechter A, Srinivasan BD. Lens epithelium and radiation cataract: I. Preliminary studies. Archives of Ophthalmology 1976; 94: 996-999.

Wu JJ, Wu W, Tholozan FM, Saunter CD, Girkin JM, Quinlan RA. A dimensionless ordered pull-through model of the mammalian lens epithelium evidences scaling across species and explains the age-dependent changes in cell density in the human lens. Journal of The Royal Society Interface 2015; 12: 20150391.

Young LK, Jarrin M, Saunter CD, Quinlan RA, Girkin JM. Non-invasive in vivo quantification of the developing optical properties and graded index of the embryonic eye lens using SPIM. Biomedical Optics Express 2018; 9: 2176-2188.

Zigman S. Effects of near ultraviolet radiation on the lens and retina. Documenta Ophthalmologica 1983; 55: 375-391.

Zintz C, Beebe DC. Morphological and cell volume changes in the rat lens during the formation of radiation cataracts. Experimental eye research 1986; 42: 43-54.

Table 1 Estimated dose rates from Japanese, Belarussian and Ukrainian lakes. The values in the table represent dose rates from artificial radionuclides.

Site	^{137}Cs sediment kBq/kg w.w.*	^{134}Cs sediment kBq/kg w.w.*	Ext. dose µGy/h	Int. dose ^{137}Cs w.w. kBq/kg	Int. dose ^{134}Cs kBq/kg	Int. dose ^{90}Sr kBq/kg	Int. dose µG/h	Total dose µGy/h
Chernobyl								
Dvorische	0.26	n.d.	Backgr.	0.19	n.d.	Not meas.	Backgr.	0.1
Gorova	0.026	n.d.	Backgr.	0.004	n.d.	Not meas.	Backgr.	Backgr.
Stoyacheye	0.75	n.d.	0.1	0.088	n.d.	Not meas.	Backgr.	0.1
Svyatoye	4.56	n.d.	0.7	6.09	n.d.	Not meas.	1.1	1.7
Glubokoye	39.7	n.d.	5.9	7.8	n.d.	13.6	9.8	15.7
Yanovsky Crawl	47.8	n.d.	7.1	2.6	n.d.	3.60	2.7	9.8
Cooling Pond	49.1	n.d.	7.3	3.0	n.d.	0.079	0.6	7.9
Fukushima								
Suzuuchi	23.2*	3.5*	4.6	3.9	0.57	Not meas.	0.86	5.5
Funasawa	32*	4.7*	6.3	3.8	0.56	Not meas.	0.83	7.1
Abukuma	35*	5.3*	7.0	0.008	0.0012	Not meas.	0.0018	7.0

* Based on sediment data from Konplev et al. (2018) and a f.w./d.w. ratio of 5.0

Figure 1. Maps showing location of sampling sites at (a) Chernobyl and (b) Fukushima. The reference dates for the radiation levels are 1986 for Chernobyl and 2011 for Fukushima.

Figure 2. Lens maximum refractive index ([ ]), focal length (mm) and radius (mm) in lakes across a gradient of contamination density at Chernobyl. Error bars show 1 Std Error (too small to be seen for refractive index).

Figure 3. Mean of cell density measurements for Lake 1; low contamination Dvorische and 2; high contamination Glubokoye; standard deviation on error bars. A t-test reveals pmean= 0.08.

Figure 4. High resolution refractive index measurements at Spring-8 showing no difference between Lake Dvorische (relatively low radiation dose; one lens from each of two perch) and Lake Glubokoye (relatively high radiation dose; 2 lenses from each of two perch).

Figure 5. A plot of the Log X-ray intensity scale against inverse space from an individual DIAMOND X-ray diffraction pattern from (a) a Lake Suzuuchi Crucian Carp lens showing a peak corresponding to the interference function which arises from the average centre to centre distance between the crystallin proteins; (b) a Chernobyl Carp lens with a dense nuclear age related cataract. The interference function has become swamped in the background radiation due to the disordering of the crystallin proteins in the lens with the age-related cataract.

Figure 6. A plot of the Bragg spacings from the central meridians of the 2D grid scans of Crucian Carp lenses from DIAMOND. Glubokoye (Open circles; “contaminated”) and Dvorische (Filled circles; “uncontaminated”). Neither Bragg spacing pattern shows evidence of protein aggregation and therefore early stage cataract formation.

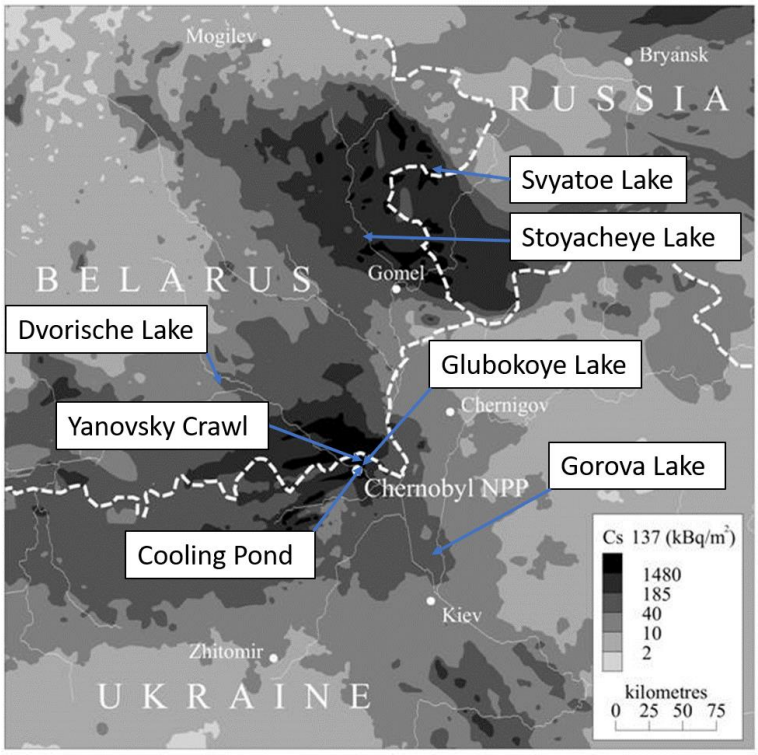

739

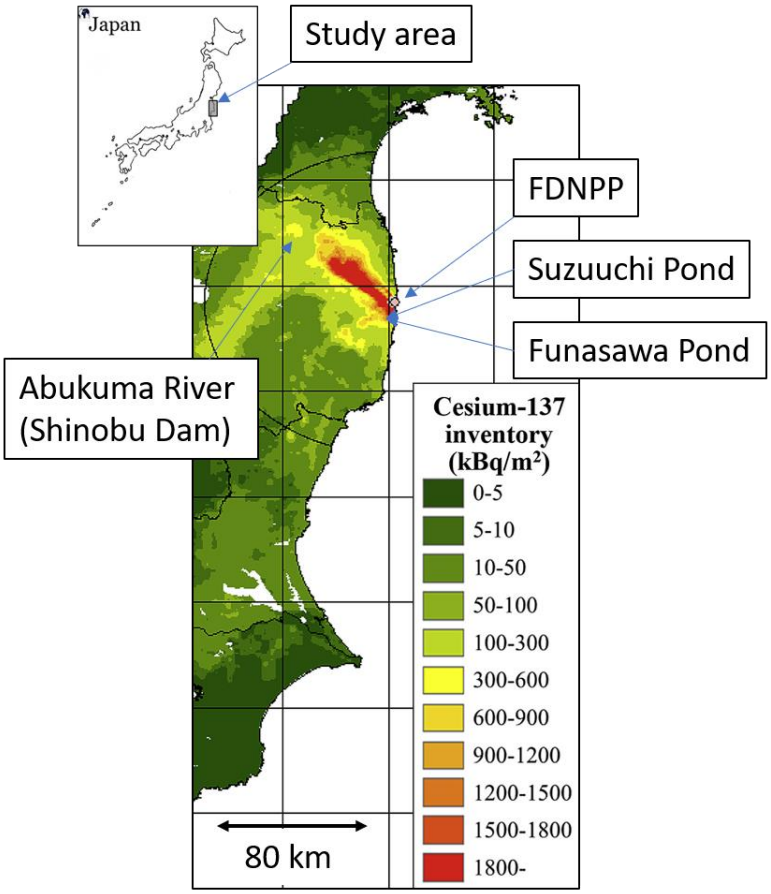

740

741 **Figure 1.** Maps showing location of sampling sites at (a) Chernobyl and (b) Fukushima. The reference dates for
742 the radiation levels are 1986 for Chernobyl and 2011 for Fukushima.

743

744

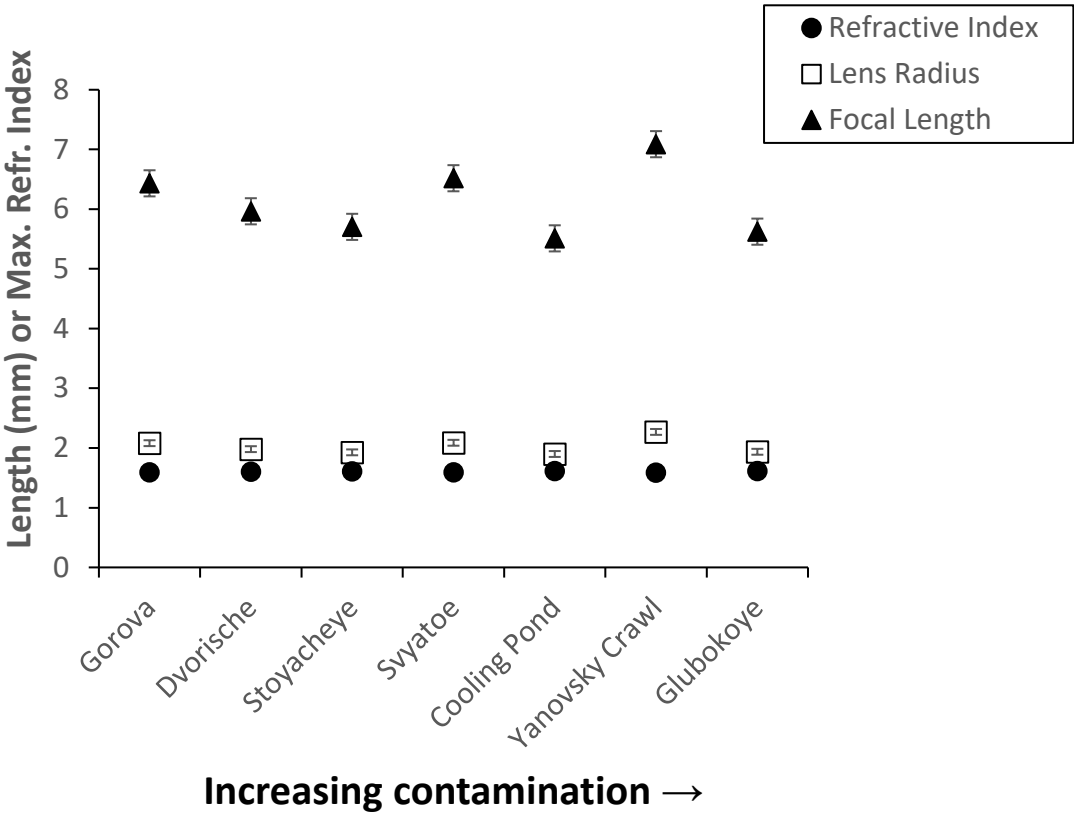

Figure 2. Lens maximum refractive index ([ ]), focal length (mm) and radius (mm) in lakes across a gradient of contamination density at Chernobyl. Error bars show 1 Std Error (too small to be seen for refractive index).

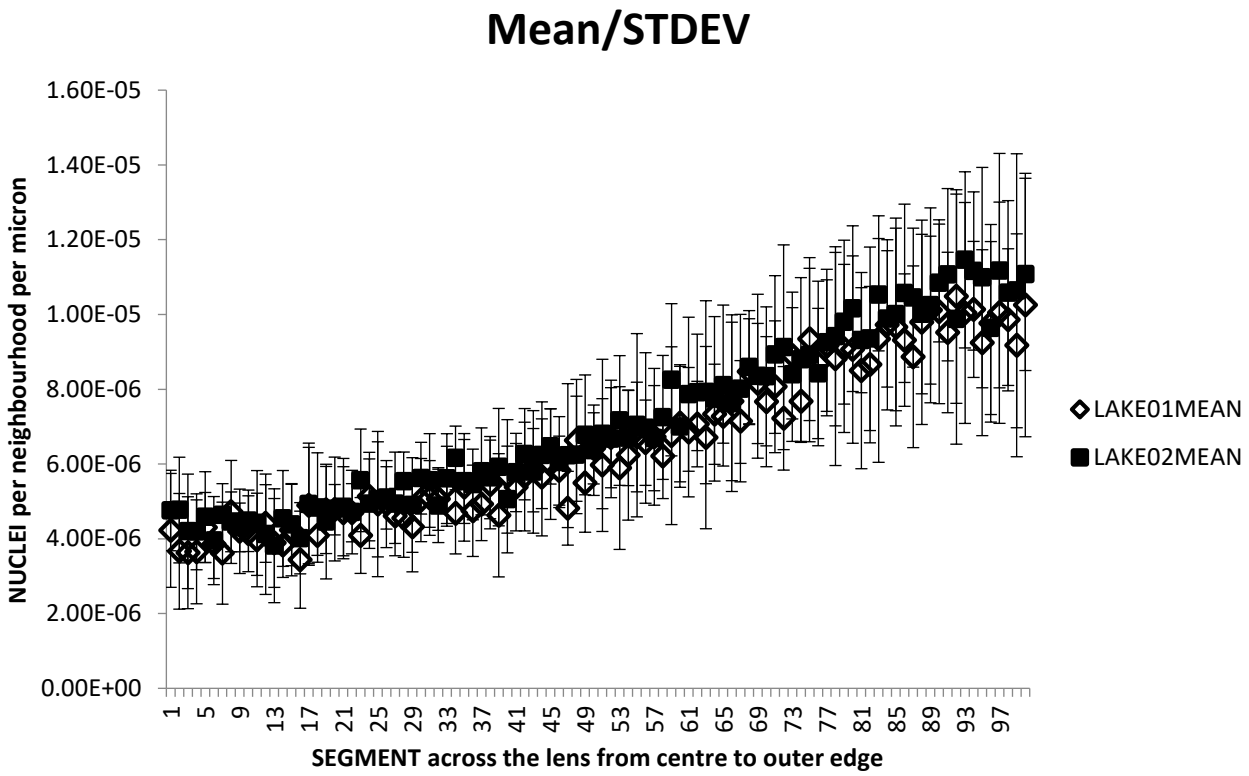

Figure 3. Mean of cell density measurements for Lake 1; low contamination Dvorische and 2; high contamination Glubokoye; standard deviation on error bars. A t-test reveals p_{mean}= 0.08.

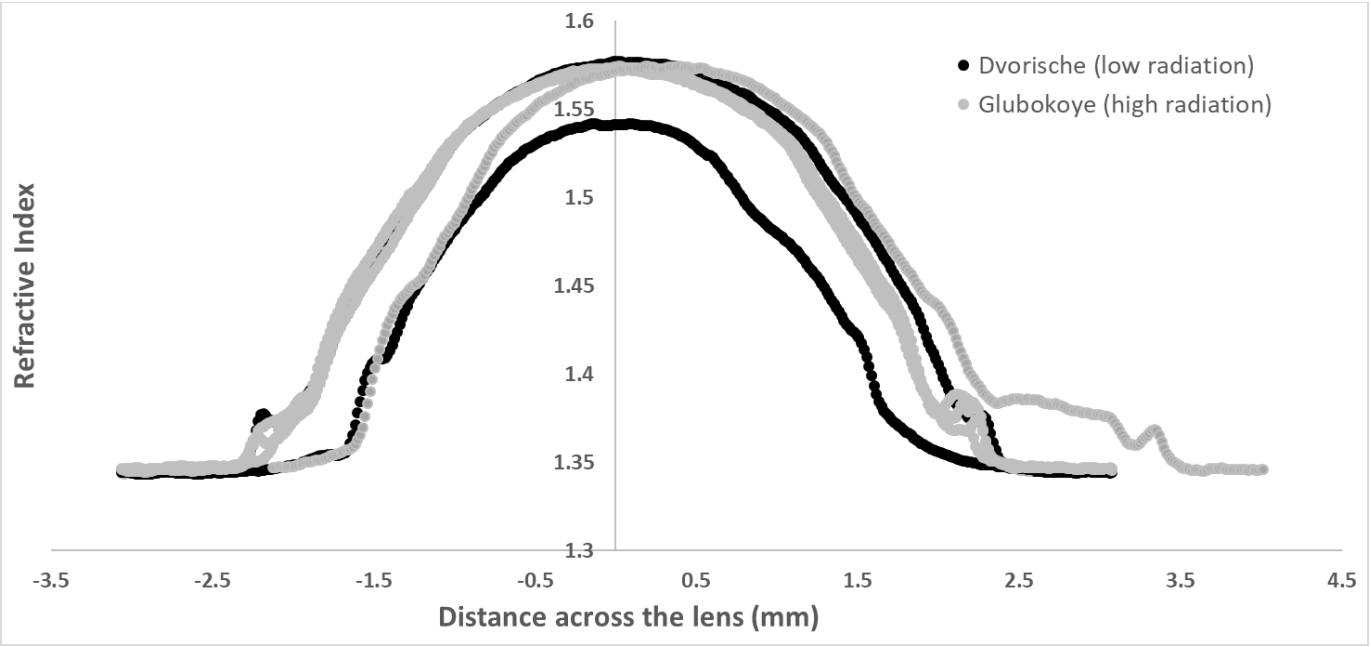

Figure 4 High resolution refractive index measurements at Spring-8 showing no difference between Lake Dvorische (relatively low radiation dose; one lens from each of two perch) and Lake Glubokoye (relatively high radiation dose; 2 lenses from each of two perch).

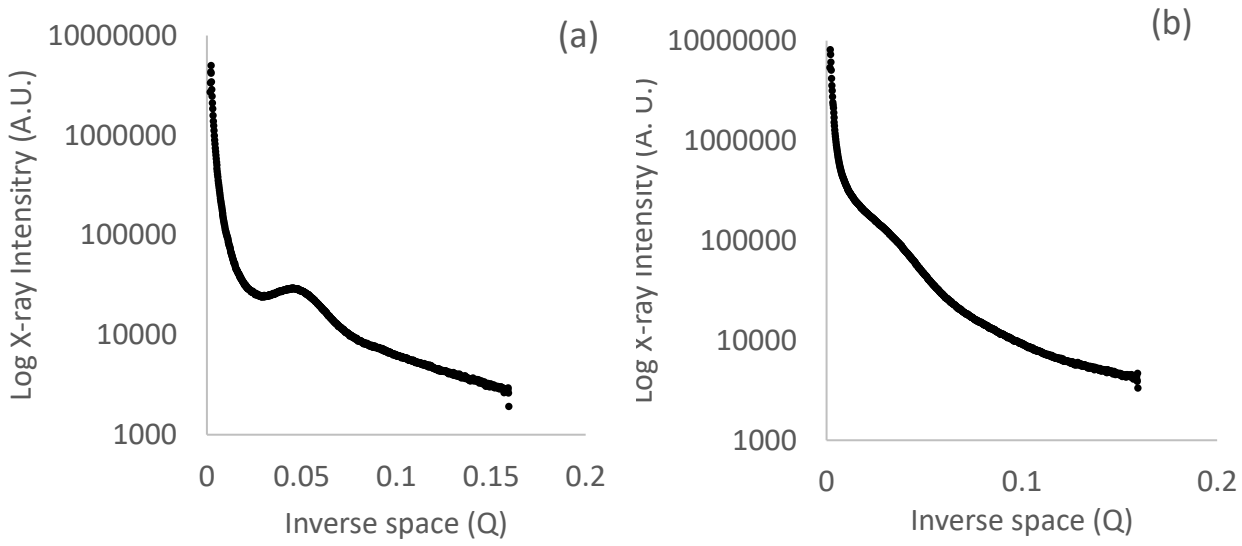

Figure 5 A plot of the Log X-ray intensity scale against inverse space from an individual DIAMOND X-ray diffraction pattern from (a) a Lake Suzuuchi Crucian Carp lens showing a peak corresponding to the interference function which arises from the average centre to centre distance between the crystallin proteins; (b) a Chernobyl Carp lens with a dense nuclear age related cataract. The interference function has become swamped in the background radiation due to the disordering of the crystallin proteins in the lens with the age-related cataract.

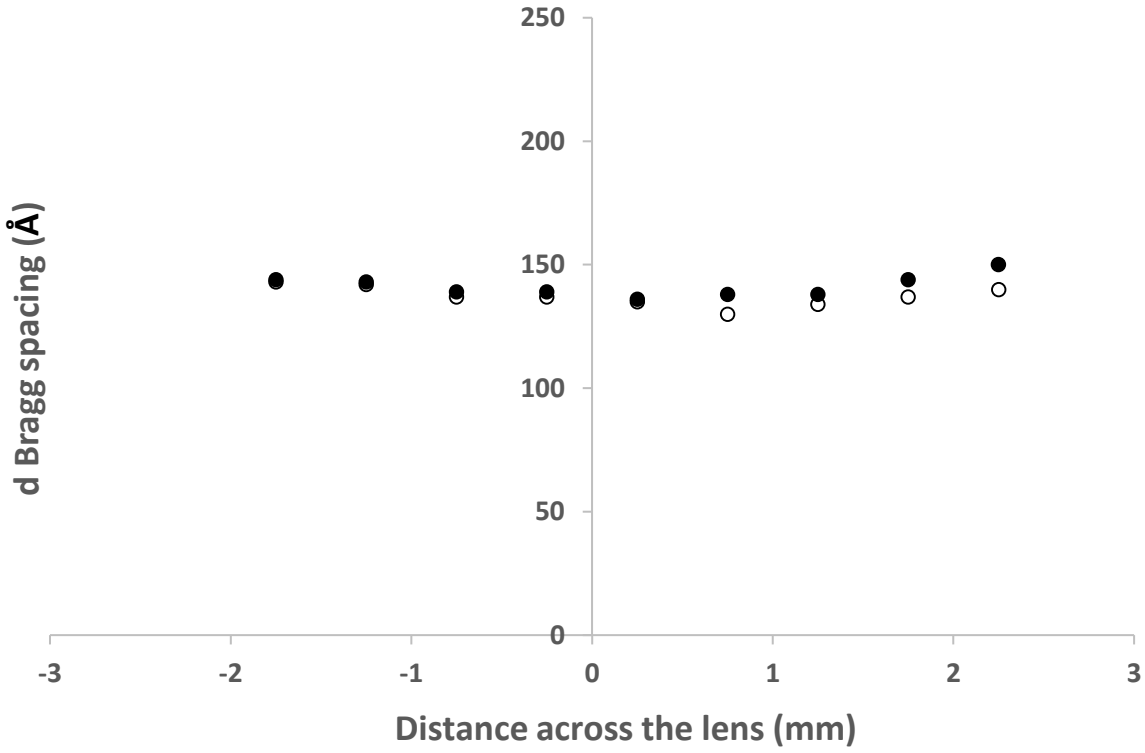

Figure 6 A plot of the Bragg spacings from the central meridians of the 2D grid scans of Crucian Carp lenses from DIAMOND. Glubokoye (Open circles; "contaminated") and Dvorische (Filled circles; "uncontaminated"). Neither Bragg spacing pattern shows evidence of protein aggregation and therefore early stage cataract formation.